All-electron Bethe-Salpeter calculations for shallow-core x-ray absorption near-edge structures

W. Olovsson,[1] I. Tanaka,[1,2] T. Mizoguchi,[3] P. Puschnig,[4] and C. Ambrosch-Draxl[4]

[1]*Department of Materials Science and Engineering, Kyoto University, Sakyo, Kyoto 606-8501, Japan*
[2]*Nanostructures Research Laboratory, Japan Fine Ceramics Centre, Atsuta, Nagoya 456-8587, Japan*
[3]*Institute of Engineering Innovation, The University of Tokyo, Yayoi, Bunkyo, Tokyo 113-8656, Japan*
[4]*Chair of Atomistic Modelling and Design of Materials, Montanuniversität Leoben, Franz-Josef-Straße 18, A-8700 Leoben, Austria*
(Received 7 December 2008; published 13 January 2009)

X-ray absorption near-edge structure spectra are calculated by fully solving the electron/core-hole Bethe-Salpeter equation (BSE) in an all-electron framework. We study transitions from shallow core states, including the Mg $L_{2,3}$ edge in MgO, the Li K edge in the Li halides LiF, LiCl, LiBr, and LiI, as well as Li_2O. We illustrate the advantage of the many-body approach over a core-hole supercell calculation. Both schemes lead to strongly bound excitons, but the nonlocal treatment of the electron-hole interaction in the BSE turns out to be crucial for an agreement with experiment.

X-ray absorption near-edge structure (XANES) is one of the most widespread spectroscopies for investigating the chemical properties of materials. It is a sensitive probe of the atomic environment, effectively measuring the transition probability between core electrons and unoccupied states. For solids featuring a band gap it is not straightforward to accurately predict the near-edge structure in the absorption spectra. In contrast to metals, where the core hole is screened very effectively by the surrounding electron cloud, bound *exciton* states can form due to the Coulomb interaction between the excited electron and the positively charged hole. Such excitonic effects are also known to have a strong influence on the overall absorption rate by modifying the oscillator strengths for transitions at higher energies. However, the methods most commonly employed to compute XANES spectra rely on the one-electron picture, thereby treating the electron and the hole as *independent*, and applying certain approximations for the hole. For instance, a core hole can be introduced at a single atom in a supercell calculation.[1,2] Other possibilities include the $(Z+1)$ approximation, where the core-ionized atom (with atomic number Z) is substituted with the next element in the Periodic Table, the introduction of a *partial* core hole (the choice of half an electron corresponds to Slater's transition state), or even the entire disregard of the hole.

More rigorously, one can go beyond the single-particle description and treat the electron-hole (e-h) interactions within many-body perturbation theory by solving the Bethe-Salpeter equation (BSE). This is motivated by the great success of the BSE approach for the optic regime. Such a BSE scheme based on the pseudopotential approximation has also been applied to x-ray absorption and related spectroscopies[3–5] emphasizing the importance of excitonic effects. For *deep* core states where the overlap between core-level wave functions on different sites can be safely neglected, indeed a close connection between the core hole and the BSE approaches has been established.[6] The electron-hole screening is described in a similar fashion in both calculations. In the former, static linear-response screening within the random-phase approximation (RPA) is utilized which is expected to be a good approximation to valence electron screening. In the core-hole approach, on the other hand, screening is treated self-consistently within the generalized gradient approximation (GGA), thus including linear as well as non-linear-response terms thereby going beyond the RPA. Nevertheless, it has been argued by Rehr *et al.*[6] that for sufficiently deep core levels both types of screening are essentially equivalent because the core state is well localized. The main difference between the two schemes could be traced back to a different treatment of the e-h exchange interaction which is local in the core-hole scheme and *nonlocal* in the BSE. While no pronounced differences were found in the results for deep core levels[6] the validity of various approximations has to be questioned for excitations from semicore states. For instance, the non-negligible overlap between valence and semicore states may also lead to electron-hole correlations which would redistribute oscillator strengths in the BSE spectra compared to the uncorrelated transitions in the supercell approach.

This is the focus of our present work where we investigate XANES spectra for *shallow* core states with transition energies well below ∼100 eV. This energy range has become increasingly important due to recent developments in experimental equipment. Electron energy-loss spectrometers (EELSs) are commonly equipped with modern transmission electron microscopes (TEMs), which are widely used by researchers in condensed-matter physics, chemistry, materials science, mineralogy, biology, etc. Shallow core edges are easier to observe than deeper edges by TEM-EELS. Improved energy resolution has led to measurements of excitonic features in the shallow edge spectra which were previously hidden. Similar progress has occurred in nonresonant x-ray Raman spectroscopy; see, for instance, the very recent experimental and theoretical work.[7,8] Such new experimental results require a sound theoretical description that can qualitatively reproduce and explain excitonic features. To this extent we employ an *all-electron* framework based on the full-potential linearized augmented plane-wave (FPLAPW) method[9] and its extension to the BSE approach[10] enabling also a comparison with core-hole calculations. Our results should serve as a benchmark since no shape approximation is made for the semicore states which are treated beyond the frozen-core approximation and thus on the same footing as valence states. In contrast, the use of pseudowave functions

and the so-called *core-valence partitioning* both commonly applied in the pseudopotential approximation could affect the core-valence interaction as has been recently demonstrated by an all-electron GW study.[11]

    We have selected three cases which have attracted considerable interest to illustrate important points in a simultaneous comparison with experiment and single-particle theory. These are the Mg $L_{2,3}$ edge ($2p$) in MgO, previously studied by several different experimental and theoretical methods,[12–15] the Li K edge ($1s$) in four Li halides, i.e., LiF, LiCl, LiBr, and LiI, representing wide band-gap insulators with well-known strong excitonic effects,[4,16–18] and finally the Li K edge in Li_2O, a material recently investigated[19–21] due to growing interest for, e.g., solid-state batteries. For these systems we evaluate the validity of different approximations in the BSE and core-hole schemes finding that a fully nonlocal treatment of the electron-hole interaction becomes important for the screening of the soft x-ray field. In other words, the BSE results turn out to be in better qualitative agreement with experimental data than the core-hole calculations unlike the situation observed for deep cores.[6]

    In brief, the Bethe-Salpeter equation represents a two-particle Schrödinger equation for the electron-hole pair,

$$\sum_{\alpha\beta\mathbf{k}} H^{e-h}_{\alpha\beta\mathbf{k},\alpha'\beta'\mathbf{k}'} A^{\lambda}_{\alpha'\beta'\mathbf{k}'} = E^{\lambda} A^{\lambda}_{\alpha\beta\mathbf{k}}, \qquad (1)$$

where H^{e-h} denotes the effective e-h Hamiltonian given by $H^{e-h} = H^{diag} + H^{dir} + 2H^{x}$. Thereby H^{diag} is the kinetic term containing the energy difference between single-particle core and empty states, and H^{dir} describes the direct e-h interaction which involves the statically screened Coulomb interaction W. Finally, H^{x} specifies the e-h exchange interaction (involving the bare Coulomb potential $\bar{v}$) which is only active for spin singlet excitations. The indices $\alpha\beta\mathbf{k}$ label core states α and unoccupied states β at a wave vector $\mathbf{k}$ inside the Brillouin zone. The eigenvalues E^{λ} in Eq. (1) are the exciton energies, while the eigenvectors A^{λ} are interpreted as coupling coefficients between the electron and the hole. Moreover, they enter the calculation of the absorption spectrum determined by the imaginary part of the dielectric tensor

$$\epsilon_2(\omega) \propto \sum_{\lambda} \left| \sum_{\alpha\beta\mathbf{k}} A^{\lambda}_{\alpha\beta\mathbf{k}} \frac{\langle \alpha\mathbf{k}|p_i|\beta\mathbf{k}\rangle}{\epsilon_{\alpha\mathbf{k}} - \epsilon_{\beta\mathbf{k}}} \right|^2 \times \delta(E^{\lambda} - \omega). \quad (2)$$

Here, $\langle \alpha\mathbf{k}|p_i|\beta\mathbf{k}\rangle$ are the transition matrix elements in the electric-dipole approximation with p_i denoting components of the momentum operator, and ϵ_{α} and ϵ_{β} are the single-particle energies for core and unoccupied states, respectively. When neglecting the direct and exchange e-h interactions in Eq. (1), Eq. (2) reduces to the RPA without crystal local-field correction, where electrons and holes are considered as independent particles. More details of our BSE approach can be found in Ref. 10 and references therein. Note that the diagonal term H^{diag} contains Kohn-Sham eigenvalues including a scissors operator shift. We use transitions above the single-particle band edge to align BSE and supercell results to the experimental spectra as indicated by the arrows in the figures. The features in the BSE spectra were converged by using an adequately dense $\mathbf{k}$ point sampling for the calcula-
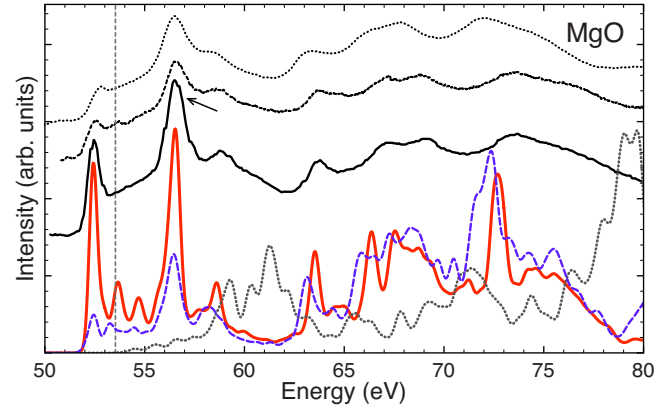

FIG. 1. (Color online) Mg $L_{2,3}$-edge spectra in MgO. From top to bottom: ELNES data from Ref. 14 with 0.7 (dotted line) and 0.3 eV (dashed line) resolution, and x-ray data from Ref. 15 (~0.2 eV resolution, full line). Theoretical results are shown below: BSE red (gray) line, supercell blue (dark gray) dashed line, and RPA dotted gray line. The vertical dashed line marks the RPA onset.

tion of the screened Coulomb interaction W as well as for the matrix elements H^{e-h}. A shifted $10\times10\times10$ $\mathbf{k}$ mesh resulting in 47 irreducible $\mathbf{q}$ points turned out to be sufficient, with the exception of LiF, where an $11\times11\times11$ mesh with 56 $\mathbf{q}$ points was used. For the computation of the screened Coulomb interaction empty states up to 272 eV above the Fermi level were considered. The number of unoccupied states β taken into account in the excitation process was 13 for MgO, 15 for LiF and LiCl, 17 for LiBr and Li_2O, and 20 for LiI. A Gaussian broadening of 0.2 eV was finally applied to the spectra. In the supercell approach, here using the WIEN2K (Ref. 9) code, the effect of the hole was simulated by explicitly introducing a core hole localized at a single atom in a supercell and adding an electron to the lowest unoccupied state to keep charge neutrality. Electron transitions were then considered at the core-ionized atom within the electric-dipole approximation. In all the calculations experimental lattice parameters were used, and exchange-correlation effects were treated within the GGA.[22]

    We start our investigation with the near-edge structure for the Mg $L_{2,3}$ edge in MgO. In the upper part of Fig. 1 experiments of different instrumental energy resolution are shown, i.e., electron energy-loss near-edge structure (ELNES) from Ref. 14 [with resolutions of 0.7 eV (dotted line) and 0.3 eV (dashed line)], which are used as a reference for the band edge, as well as soft x-ray reflection spectroscopy (full line, resolution of ~0.2 eV).[15] The red (gray) line denotes the BSE result, the dashed blue (dark gray) line the 128 atom supercell calculation, while the dotted gray line corresponds to the RPA without local-field corrections. Studying the experimental spectra it is interesting to note that the edge peak around 52.5 eV becomes more distinct with increasing resolution. The difference between the BSE and RPA results reveals that this feature corresponds to a strong core exciton. This is a clear demonstration of the importance of excitonic effects in the near-edge structure. Comparing the BSE with the supercell spectrum, we observe an overall similarity between these two computational approaches, and both schemes roughly agree for the position of the edge peak. The
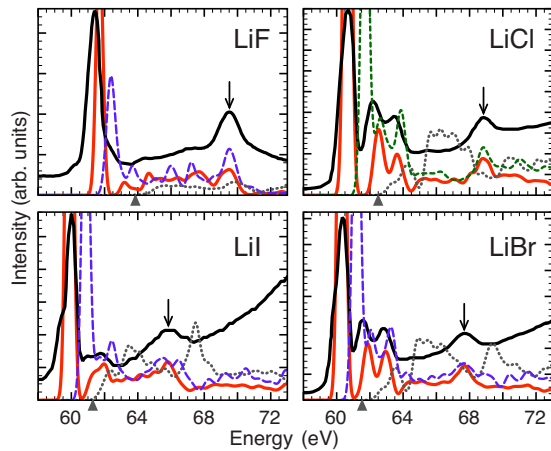
FIG. 2. (Color online) The Li K edge in the lithium halides LiF, LiCl, LiBr, and LiI comparing experiment (full line) (Ref. 18) and theoretical results; BSE red (gray) line, DFT calculations for 64 atoms dashed blue (dark gray) line and in the case of LiCl 128 atoms short-dashed green (dark gray) line, and RPA dotted gray line. The triangles mark the RPA onset.

gross accordance of the two approaches suggests that a *local* treatment of the electron-hole exchange interaction is a valid approximation for the Mg $L_{2,3}$ edge. Indeed, we find only a minor influence of the spectra on the exchange term H^x for the L edge. For the deep core, i.e., the Mg K edge, many-body theory and core-hole calculations were shown to be in excellent agreement with each other.[6] Here we find, however, that the BSE theory performs better. For instance, the intensity ratio of the first two prominent peaks is in better agreement with the high-resolution measurements compared to the supercell result. Since the static dielectric constant is found to be the same in both approaches, we conclude that the nonlocal treatment of the direct term in the BSE leads to the observed redistribution of oscillator strength.

In Fig. 2 we present results for the Li K edge in the Li halides, starting from LiF in the upper left corner and clockwise, LiCl, LiBr, and LiI, respectively. BSE results, red (gray) lines, are compared with FPLAPW core-hole calculations using 64 atom supercells, dashed blue (dark gray) lines. In the case of LiCl a result for 128 atoms, short-dashed green (dark gray) line, is displayed. Experimental values (full lines) are from a recent XANES study.[18] The interpretation of the near-edge spectra in the Li halides has received much attention over the years.[4,16,17] There are strong excitonic effects as has already been noted by previous work based on a pseudopotential method.[4] The four spectra in Fig. 2 reveal pronounced edge peaks, due to p-like core excitons, followed by a detailed fine structure. In general, the BSE results follow the experiment more closely than the core-hole calculations. In particular, the energy positions of the edges are considerably overestimated by the supercell calculations, while the BSE spectra are in very good agreement with experiment. For the Li K edges we find a pronounced influence of the exchange term on the energetic position of the edge peak, and the proper nonlocal treatment of the e-h exchange interaction proves to be important. This is because the exchange integrals between an s-symmetry semicore state and

a valence state give a non-negligible contribution as opposed to the situation for the L edge in MgO discussed above. Moreover, also the e-h correlations introduced by the nonlocality of the direct term in the BSE can be made responsible for giving the correct exciton binding energy and shifting oscillator strength toward the exciton peak. Upon closer look, additional weak pre-edge structures can be found in the experiments. These are usually ascribed to vibrational effects, which are not included in the present calculations. However, we note that breaking the symmetry of the crystal lattice by a small distortion of the atomic positions enables transitions to lower energy s-like states and hence leads to similar features.

The present methodology of the Bethe-Salpeter equation also allows for an evaluation of the real-space exciton wave function, constructed from the single-particle electron and hole wave functions and the coupling coefficients, $\Phi^\lambda(\mathbf{r}_e, \mathbf{r}_h) = \Sigma_{\alpha\beta\mathbf{k}} A^\lambda_{\alpha\beta\mathbf{k}} \psi^*_{\alpha\mathbf{k}}(\mathbf{r}_h) \psi_{\beta\mathbf{k}}(\mathbf{r}_e)$.[10] In Fig. 3(a), we give a demonstration for the Li K edge in the rocksalt structure LiCl for one of the degenerate p-like core excitons. Note that the energetically lowest exciton has s-like symmetry and exhibits effectively zero oscillator strength. (To verify this finding, a denser $\mathbf{k}$ mesh was applied.) The core exciton is well localized in between the holed Li atom and the two nearest Li neighbors. We can compare this exciton wave function resulting from the BSE approach to the single-electron wave function of the supercell scheme for the unoccupied p state in the presence of a core hole [Fig. 3(b)]. The striking similarity between the two approaches shows that this p state is dominating the final states in the excitation process, and that the differences in the exciton binding energy hardly affect the extension of the electron-hole pair.

In our last example we turn to the Li K edge in Li$_2$O, Fig. 4. Theory and ELNES experiment[21] are shown with the same denotation as in Fig. 2. A 96 atom supercell was used for the core-hole calculation. On the basis of ground state and core-
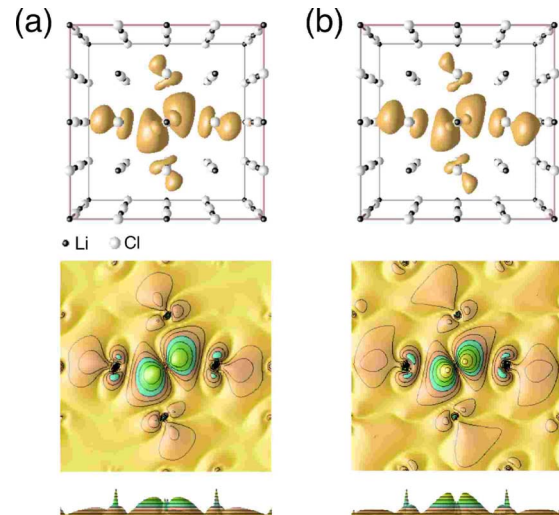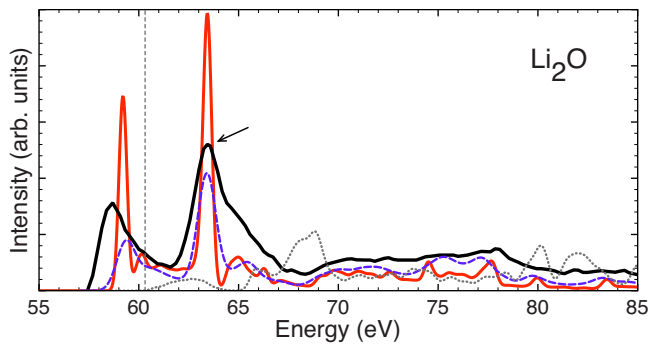

FIG. 3. (Color online) The exciton wave function for the Li K edge in LiCl. (a) Absolute value of the electron distribution with the hole at the central Li atom for the lowest p-like core exciton (BSE). (b) Unoccupied p state in a 64 atom supercell calculation. Contour lines on the (001) planes are shown below.

FIG. 4. (Color online) The Li K edge in Li_2O. Same notation as Figs. 1 and 2.

hole DFT calculations it was argued in Ref. 20 that the two pronounced peaks in the spectra are related to excitons. Indeed, our BSE result clearly identifies the edge peak as core exciton. As for the K edges in the lithium halides the nonlocal treatment of the exchange is important and electron-hole correlations further modify the shape of the spectra close to the edge. Again, the better agreement of the BSE spectra with experiment underpins the need for this more elaborate treatment of the e-h interaction in the XANES spectra of semicore states.

In summary, we have investigated XANES spectra of dif-

ferent compounds with shallow core states by solving the BSE in the framework of the all-electron FPLAPW method. Our method does neither employ the frozen-core approximation nor rely on any shape approximation of semicore wave functions allowing us to describe them on an equal footing as valence states. Thus, our results set a benchmark for the first-principles treatment of XANES spectra. They clearly demonstrate that the BSE improves over core-hole calculations, especially in the case of the Li K edges in the wide band-gap lithium halides, with a smaller difference for Li_2O, and a better intensity ratio for the Mg $L_{2,3}$ edge in MgO. Both the BSE and the core-hole methods lead to bound excitons, but the BSE turns out to be important for an agreement with experiment. While the electron-hole screening is rather similar in the BSE and core-hole approach, the nonlocality of the direct term in the BSE introduces weak electron-hole correlations which shift oscillator strength toward the exciton peak. Moreover, we find the nonlocal treatment of the exchange in the BSE to be preferable over the local approximation used in the core-hole method.

[1] I. Tanaka, T. Mizoguchi, and T. Yamamoto, J. Am. Ceram. Soc. **88**, 2013 (2005).

[2] T. Mizoguchi, I. Tanaka, S. Yoshioka, M. Kunisu, T. Yamamoto, and W. Y. Ching, Phys. Rev. B **70**, 045103 (2004).

[3] E. L. Shirley, Phys. Rev. Lett. **80**, 794 (1998).

[4] E. Shirley, J. Electron Spectrosc. Relat. Phenom. **137–140**, 579 (2004).

[5] J. A. Soininen and E. L. Shirley, Phys. Rev. B **64**, 165112 (2001).

[6] J. J. Rehr, J. A. Soininen, and E. L. Shirley, Phys. Scr. **T115**, 207 (2005).

[7] Y. Feng, J. A. Soininen, A. L. Ankudinov, J. O. Cross, G. T. Seidler, A. T. Macrander, J. J. Rehr, and E. L. Shirley, Phys. Rev. B **77**, 165202 (2008).

[8] T. T. Fister, G. T. Seidler, E. L. Shirley, F. D. Vila, J. J. Rehr, K. P. Nagle, J. C. Linehan, and J. O. Cross, J. Chem. Phys. **129**, 044702 (2008).

[9] P. Blaha, K. Schwartz, G. Madsen, D. Kvasnicka, and J. Luitz, *WIEN2k An Augmented Plane Wave Plus Local Orbitals Program for Calculating Crystal Properties* (Vienna, Austria, 2001).

[10] P. Puschnig and C. Ambrosch-Draxl, Phys. Rev. B **66**, 165105 (2002).

[11] R. Gómez-Abal, X. Li, M. Scheffler, and C. Ambrosch-Draxl, Phys. Rev. Lett. **101**, 106404 (2008).

[12] T. Mizoguchi, I. Tanaka, M. Yoshiya, F. Oba, K. Ogasawara, and H. Adachi, Phys. Rev. B **61**, 2180 (2000).

[13] M. Stener, G. Fronzoni, and R. D. Francesco, Chem. Phys. **309**, 49 (2005).

[14] T. Mizoguchi, K. Tatsumi, and I. Tanaka, Ultramicroscopy **106**, 1120 (2006).

[15] W. L. O'Brien, J. Jia, Q.-Y. Dong, T. A. Callcott, J.-E. Rubensson, D. L. Mueller, and D. L. Ederer, Phys. Rev. B **44**, 1013 (1991).

[16] S. T. Pantelides and F. C. Brown, Phys. Rev. Lett. **33**, 298 (1974).

[17] S. T. Pantelides, Phys. Rev. B **11**, 2391 (1975).

[18] K. Handa, K. Kojima, K. Ozutsumi, K. Taniguchi, and S. Ikeda, Memoirs of the SR Center Ritsumeikan University **7**, 3 (2005).

[19] J. Tsuji, H. Nakamatsu, T. Mukoyama, K. Kojima, S. Ikeda, and K. Taniguchi, X-Ray Spectrom. **31**, 319 (2002).

[20] N. Jiang and J. C. H. Spence, Phys. Rev. B **69**, 115112 (2004).

[21] V. Mauchamp, F. Boucher, G. Ouvrard, and P. Moreau, Phys. Rev. B **74**, 115106 (2006).

[22] J. P. Perdew, K. Burke, and M. Ernzerhof, Phys. Rev. Lett. **77**, 3865 (1996).